Modelling of Thermodynamic, Thermophysical and Physical Properties of Lead-Free Solder Alloys

Zhanli Guo*, Nigel Saunders, Peter Miodownik, Jean-Philippe Schillé
Sente Software Ltd.
Surrey Technology Centre, The Surrey Research Park, Guildford, Surrey, U.K.
* z.guo@sentesoftware.co.uk

Abstract

The demand for new and improved lead-free solder (LFS) alloys grows steadily as the need for reliable lead-free electronic products increases. Thermodynamic calculations have proved to be an important tool in providing information for the design and understanding of new LFS systems. However, such tools often fall short from directly providing the information that is actually required by the end users, such as physical and thermophysical properties. In the present work, models have been created such that a full set of such properties can be calculated for solder alloys for the multi-component system Sn-Ag-Al-Au-Bi-Cu-In-Ni-Pb-Sb-Zn. The properties, given for both the overall alloy or for each phase if required, include coefficient of thermal expansion, densities, various modulii, thermal conductivity, liquid surface tension and viscosity, all as a function of composition and temperature (extending into the liquid state).

Introduction

To meet the requirements arising from environmental and health issues concerning the toxicity of lead, lead-free solder (LFS) alloys have been developed during the past decade to replace conventional Pb-Sn alloys. Studies on LFS materials were particularly accelerated in the last years due to the introduction of RoHS (*Restriction of Hazardous Substances*) Directive on 1 July 2006, i.e. all electrical and electronic products in the EU market must now pass RoHS compliance.

Although many industries serving the information communications technology and consumer electronics have claimed their production has been completely redesigned to accommodate the newly developed LFS alloys, the long term effect of such a switch remains to be seen. It has become clear though that the cost, and increased risk, to industry is significantly greater that initially thought, and to close the remaining knowledge gaps could take several more years of investment and investigation. Therefore, interest in developing new LFS alloys will remain, if not increase, both for improved performance, reliability and to reduce toxicity.

As part of the process of developing new LFS alloys, thermodynamic calculations have been extensively reported [1,2,3,4,5] and a number of thermodynamic databases have been developed specifically for this purpose [1,2]. However, the limitations of a purely thermodynamic approach are well known, in that it does not provide direct information for general material properties, such as physical, thermophysical and mechanical properties, which are the key to the application of any new solders. Such material properties are also critical inputs for the manufacturing and reliability modelling of soldered components using finite element (FE) or finite difference (FD) tools.

In recent years, the modelling and calculation of a wide range of material properties has become possible, due to the development of the JMatPro software [6]. To date, the application of this software has been mainly in the area of structural metallic alloys [7,8,9,10]. However, many of the requirements for material properties in solders are identical and the scientific basis for modelling solders is very similar. In particular, much of the development work for JMatPro is aimed at providing reliable material properties at temperatures approaching the melting point (T_m), which is a basic requirement for even the room temperature (T_0) properties of Sn-based solder alloys where T_0/T_m is usually of the order 0.6.

The present paper reports recent progress made in extending JMatPro for use in Sn-based solder alloys. The status of thermodynamic calculations will be first briefly reviewed and discussed, then the extension to calculation physical properties, such as expansion coefficients, modulii, and surface tension of the liquid will described, with emphasis on their use for multi-component solder alloys.

Thermodynamic Modelling

The use of CALPHAD (Calculations of Phase Diagrams) approach is well established [11,12] and the requirements to produce successful thermodynamic databases for use with multi-component alloys have been discussed in detail [12]. The current thermodynamic database includes the following elements:

Sn-Ag-Al-Au-Bi-Cu-In-Ni-Pb-Sb-Zn

It should be noted that although the database was designed and tested for Sn-based alloys, the coverage of binary and ternary systems allows it to be used at compositions where Sn may not be the major element. The database has been constructed by combining thermodynamic assessments of binary and ternary systems obtained from the open literature alongside extensive new work. The database includes a complete coverage of binary assessments, and a wide range of ternary assessments including all Sn-X-Y systems.

It should be noted that models and critical thermodynamic parameters from various published thermodynamic assessments in the literature may differ. For example, models for important phases may not be compatible and lattice stabilities for metastable crystal forms of the elements may not be the same. Therefore, as part of the new database creation, self-consistent models for all phases and Gibbs energy functions for the pure elements were used. In a substantial number of cases, where otherwise good thermodynamic assessments were reported, re-modelling of key phases, such as those based on the B8 type phases, which

include Cu_6Sn_5 and AuSn, was undertaken to provide internal self-consistency.

A basic requirement for a candidate solder alloy to replace a Pb-containing solder is to have a specific freezing range, the temperature range over which both solid and liquid co-exist; this freezing range is dictated by the application. To replace the Pb-Sn eutectic solder, the ideal alloy would be eutectic or near-eutectic, with a liquidus temperature low enough to avoid damaging components and a solidus temperature high enough to maintain joint reliability during thermomechanical fatigue. The database has been tested extensively against experimental solders and Fig.1 shows a comparison plot for solidus and liquidus values for solder alloys reported in the NIST solder alloy property database [13] (see Table 1 for details).

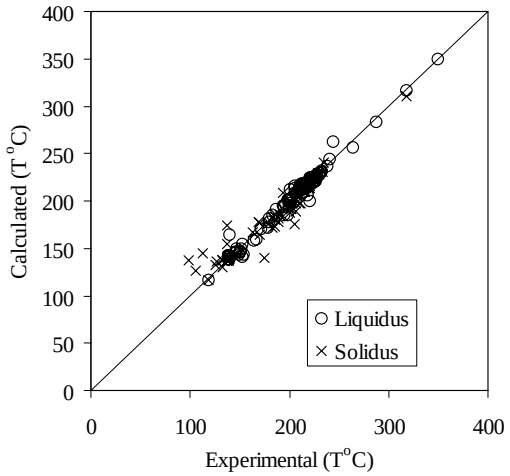

Fig. 1: Comparison between experimental [13] and calculated liquidus and solidus temperatures for various solder alloys

Table 1. Composition range and number of alloys used in Fig.1

Element	max level (wt%)
Sn	Balance
Ag	7
Bi	58
Cu	4
In	52
Pb	97
Sb	8
Zn	9
Total number of alloys	120

In certain cases, particularly those with higher levels of Cu and Ag additions, intermetallics may control the liquidus. However it is clear from the main source of data (Table 4.1 of Ref. 13) that the liquidus quoted is almost certainly for the temperature when Sn first forms and the calculated results are therefore given for this case. The most likely reason that the temperature for Sn formation appears in the tables of Ref. 13 is that this is a strong reaction, with a highly visible thermal signature. On the other hand the formation of minor amounts of intermetallic compound has a very small thermal signature, particularly when liquidus slopes are steep, as is the case for (Cu,Ag)-Sn compounds.

Physical Property Modelling

Thermophysical and physical properties are an important part of materials science, particularly at the present time when such data is a critical input for software programmes dealing with process modelling. A major achievement of the JMatPro software project has been the development of an extensive database for the calculation of such properties which can be linked to its thermodynamic calculation capability. For each individual phase in multi-component systems, properties, such as molar volume, thermal conductivity, Young's modulus, and Poisson's ratio, are calculated using simple pair-wise mixture models.

$$P = \sum_i x_i P_i^o + \sum_i \sum_{j>i} x_i x_j \sum_v \Omega_{ij}^v (x_i - x_j)^v \qquad (1)$$

where, P is the property of the phase, P_i^0 is the property of the phase in the pure element, Ω_{ij}^v is a binary interaction parameter dependent on the value of v, x_i and x_j are the mole fractions of elements i and j in the phase. Both P_i^0 and Ω_{ij}^v are temperature dependent and it is possible to include ternary or higher order effects where appropriate.

Once the property of each individual phase is defined, the property of the final alloy can be calculated using appropriate mixture models [14,15,16]. Utilising well established relationships between certain properties (e.g. thermal and electrical conductivity), reduces the need for individual databases for each property. At present the properties that can be modelled include: volume, density, thermal expansion coefficient, Young's, bulk and shear modulii, Poisson's ratio, thermal conductivity and diffusivity, electrical conductivity and resistivity, viscosity and diffusivity of the liquid. The physical property models have been extensively tested and validated, particularly for solidification purposes [17].

Extensive work has been undertaken to build up and

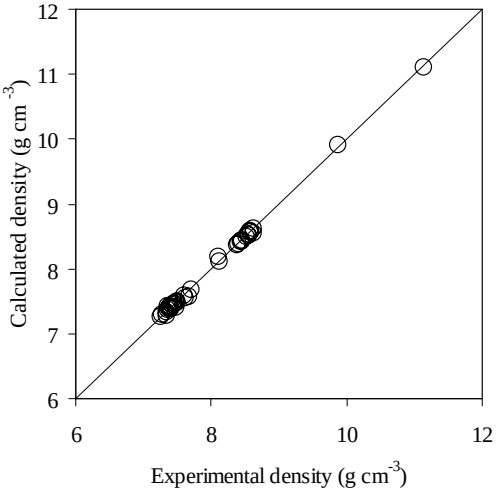

Fig. 2: Comparison between experimental [13] and calculated densities of various solder alloys

validate the requisite property databases for solder systems. Comparison of experimental and calculated densities for many solder alloys are shown in Fig.2 where the source of experimental data is again the NIST property database.

While calculations of room temperature properties such as density are relatively commonplace, all properties calculated by JMatPro are temperature dependent and are calculated into the liquid state. The related calculation to density is the coefficient of thermal expansion (CTE) and the temperature dependence of the CTE. Fig.3 shows the calculated CTE of a solder alloy Sn-3.9Ag-0.6Cu (in wt%) in comparison with experiment [18]. Fig.4 shows the calculated Young's Modulus in comparison with experiment. In these two figures, the symbols "#1" and "#2" denote two alloys of the same type, whereas "As cast" or "Aged" were the condition of the alloys tested.

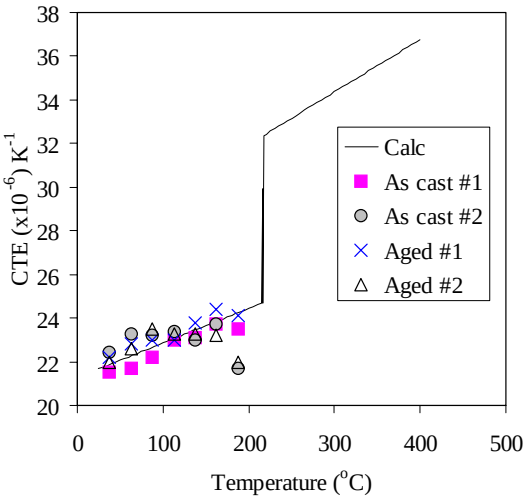

Fig. 3: Comparison between experimental [18] and calculated CTE of Sn-3.9Ag-0.6Cu solder alloy

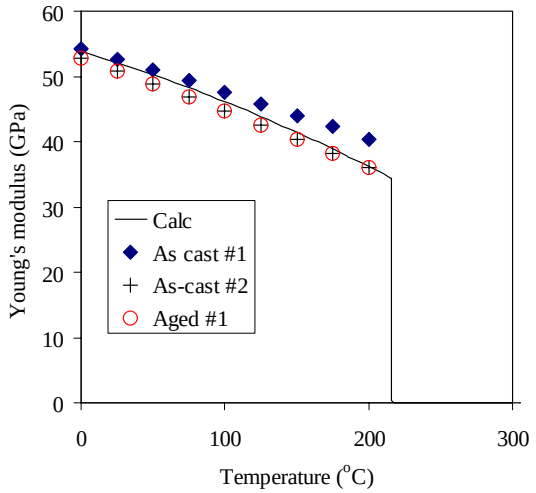

Fig. 4: Comparison between experimental [18] and calculated Young's modulus of Sn-3.9Ag-0.6Cu solder alloy

While the properties mentioned above are very important, it is also necessary to consider surface tension of solder alloys. For instance, surface tension is critical input for the modelling of many steps in manufacturing such as solder paste printing, solder bump solidification and solder joint shape.

A theoretical treatment for binary alloys developed by Butler [19] has been used by numerous authors and has been well substantiated over the years [20,21,22,23]. However there has been much less work on devising an extension capable of handling multi-component alloys. The basic expression derived by Butler is as follows:

$$\sigma = \sigma_i^{[T]} + \frac{RT}{A_S}\ln(a_i^* / a_i) \qquad (2)$$

where $\sigma_i^{[T]}$ is the surface tension of pure component i at temperature T, A_S is the molar surface area, a_i is the activity of component i (at temperature T) and a_i^* is the activity of component i in a monomolecular layer at the surface. A_S can be calculated via the molar volume $V_{m(i)}$ of the species via:

$$A_s = LN^{1/3}V_{m(i)}^{2/3} \qquad (3)$$

where N is Avogadro's number and L is a constant reflecting the packing of atoms in the surface. Therefore, the three basic ingredients for any calculation of the surface tension of alloys are,

(i) values for the surface tension (σ_i) of the pure elements,
(ii) the molar volume ($V_{m(i)}$) as a function of composition,
(iii) the activities (a_i^* and a_i) of the alloying components (i).

The activities have traditionally been expressed in terms of excess Gibbs energy parameters for the bulk liquid and corresponding values for a surface phase with a different number of nearest neighbours, which reflects the need to adjust bond angles and strength at the liquid-vapour interface). It has been generally assumed that $\ln(a_i^*)$ is linearly proportional to $\ln(a_i)$ with the constant of proportionality β related to the ratio of the number of nearest neighbours in the surface layer Z^* to the equivalent number Z in the bulk of the liquid.

Since values for M_v and a_i are already available from JMatPro, it is only necessary to evaluate the surface tension of the elements in the liquid state to calculate the surface tension for alloys. The results for binary alloys give a good match

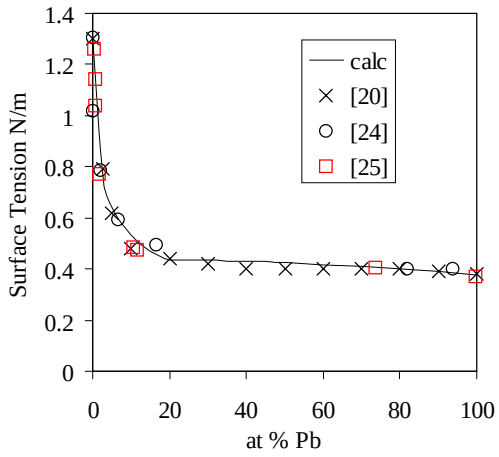

Fig.5: Comparison between calculated, experimental [24,25] and previous calculation [20] of liquid surface tension in Cu-Pb alloys at 1100ºC.

both with experiment [24,25] and in comparison with calculations from other groups [20] (Fig.5).

The reason why ternary and higher order alloys have only been considered relatively recently is because there is a marked increase in the number of input parameters and various workers have taken different approaches to this problem, see for example Pajarre et al. [26] and Tanaka and Iida [27]. For systems that are relatively ideal, the precise method adopted does not make much difference. However in the general case there can be appreciable changes in activity from ideal and thermodynamic calculation is required for any approach to be predictive.

Experimental surface tension data for ternary or higher order systems is rather sparse. Pajarre et al [26] only applied their treatment to Ag-Au-Cu and there are some earlier results for Fe-Ni-Cr [28]. Ternary data exists for solder systems such as Sn-Ag-Sb [3] and Sn-Ag-In [29], but these only contain relatively low levels of ternary additions because of the constraint of meeting melting point and freezing range requirements. Here again there is a great potential within JMatPro for the development of figures of merit incorporating combinations of such parameters.

Our approach is also based on the Butler equation, but differs in detail on how it is extended to higher order systems [30]. The general accuracy achieved by JMatPro is illustrated in (Fig. 6) which shows that the accuracy for ternary alloys is on par with that achieved for binary systems. One immediate advantage of such calculations is in making choices about trend lines. In the absence of calculated values, it is very difficult to make a judgment about the validity of some of the fluctuations reported in the literature. The general accuracy attained also gives confidence in predicted results for systems for which no experimental results are available and one of the potential uses is in the prediction of wettability, through using Young's equation.

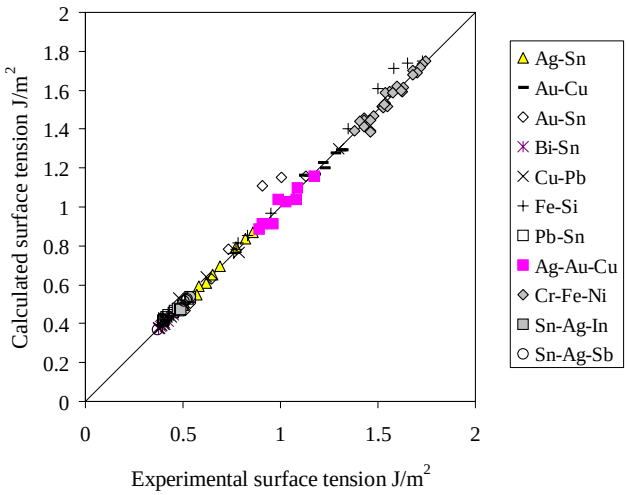

Fig.6: Comparison between experimental and calculated liquid surface tension for various binary and ternary alloys

Solidification Properties

The solidification process of solders is also an important factor in the design of LFS alloys. One limiting case for describing solidification behaviour is solidification obeying the lever rule (thermodynamic equilibrium). For equilibrium solidification it is assumed that at each temperature during cooling, complete diffusion occurs in the solid as well as in the liquid and, therefore, all phases are in thermodynamic equilibrium at each temperature.

However, in reality, solidification usually occurs via a non-equilibrium route. Since the degree to which non-equilibrium solidification occurs is determined by kinetic factors, it is difficult to predict the phase evolution during solidification. The limiting case describing this solidification behaviour is the Scheil path, where diffusion in the solid is forbidden and thermodynamic equilibrium exists only as local equilibrium at the liquid/solid interface. This predicts the most extreme microsegregation with the lowest final freezing temperature. Although a full model for solidification behaviour requires the incorporation of a kinetic analysis of micro-segregation and back diffusion, the predictions of the Scheil model are close to reality for many alloys for the time scales found in soldering.

A solidification simulation was carried out for a promising alternative alloy to Pb-Sn solders, the Sn-2.0Ag-0.5Cu-7.5Bi (wt%) alloy shown in Fig. 7(a). The equilibrium calculation is given for comparison in Fig. 7(b). In both cases, solidification starts with small amounts of primary crystals of

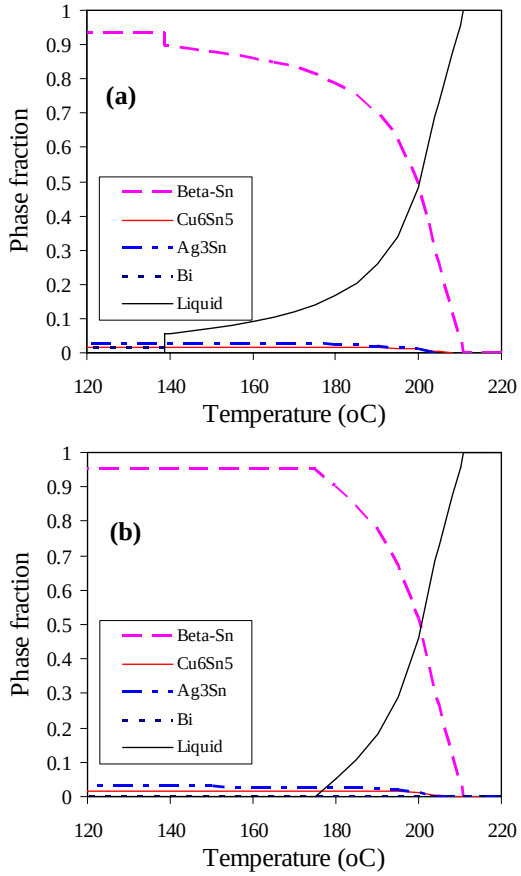

Fig.7: A solidification simulation of the Sn-2.0Ag-0.5Cu-7.5Bi alloy (a) Scheil model, and (b) equilibrium calculation

η-Cu_6Sn_5. However, the liquid phase disappears at 174.8°C under the equilibrium conditions, whereas according to the Scheil model, solidification ends at 138.9°C in correspondence with the eutectic reaction of the Sn-Bi system.

Discussion

The worldwide movement in the electronics industry to implement lead-free solders has created a need for fundamental data that accurately describe the behaviour of these alloys in solder joints and which can be used to develop appropriate reliability models. Although tremendous efforts have been made in this direction, there is still a definite lack of material data for LFS alloys. Most of the available references focus on data collected via experimental routes that are costly and time-consuming. Moreover, the fact that a large number of experiments are required to generate sufficient data to cover the multitude of proposed alloy types/compositions and conditions means experimentation is not always an option. Existing computer modelling work is normally based on finite-element analysis, dealing with real production and reliability issues. Although materials properties are critical inputs for such types of modelling, little work has been done on computer modelling the whole range of materials properties as a function of phase distributions calculated thermodynamically in real time.

It should be noted that the work reported here contains only examples of the modelling of some thermophysical and physical properties for solders. The modelling of mechanical properties is in progress, a step which will bring the range of properties to the same level as for other materials systems already treated by JMatPro. Today's electronics industry is a severely competitive place. So any technique that helps to rapidly evaluate alternative alloy compositions and highlight potential ways of reducing cost could offer companies considerable advantages (see Appendix Table I).

The scatter of the experimental data in literature is better described as erratic rather than random since few of the reported studies were statistical in nature. The thermal and/or deformation history of the sample is rarely recorded, and the microstructural features of the specimens are not always available. The fact that room temperature is close to 60% of the melting temperature for most of the solder alloys means it is effectively "high temperature", making the microstructure unstable even during experiments. Getting a better idea of the significance of several variables may also benefit the development of testing standards for solder alloys.

Summary and Future Work

Work has been reported on the extension of the Materials Property Software, JMatPro, for application to solder alloys. Thermodynamic, thermo-physical and physical properties of solder alloys have been calculated and results validated against experiment. Surface tension calculations have been made and applied to both binary and higher order alloys. Work is on-going concerning the extension of the surface tension calculations to wettability, as this is the ultimate requirement. Work is also currently being undertaken to extend JMatPro's capability for calculating high temperature mechanical properties in structural alloys to include solder alloys, so that flow stress as a function of temperature and strain rate can be calculated up to the melting point and into the mushy zone.

Acknowledgments

ZG and NS wish to thank Mr. N. Hoo at Tin Technology (U.K.) for useful discussions.

Appendix

In February 2001, a workshop on Modeling and Data Needs for Lead-Free Solders was held in New Orleans, L.A. The report summary of this workshop [31] described the scientific needs by the microelectronics community, and has been serving as a roadmap for research in the reliability of lead-free solders. The information on the priority level for various material properties given in Table I was taken from this report for Sn-3.9Ag-0.6Cu, Sn-0.7Cu, Sn-3.5Ag and Sn-37Pb (all in wt%) solder alloys. The present capabilities of JMatPro on property modelling is shown in Table I as well, together with JMatPro's planned development in near future.

Table I, Industrial list of priorities of materials properties

CTE (liquid and solid state)	1	*
Volume Change on freezing (liquid and solid state)	1	*
Specific Heat	3	*
Latent Heat	3	*
Thermal Diffusivity	3	*
Thermal Conductivity	3	*
Electrical Conductivity/Resistivity	3	*
Surface Tension at temp of solder	2	*
Wettability	2	**
Shear Strength (strain rates (SRs) from 10^{-1} to 10^{-6} s^{-1})	1	**
Ring in Plug (SRs from 10^{-1} to 10^{-6} s^{-1})	3	
E (Young's modulus) at 25°C	1	*
E at 50, 100 and 125°C	1	*
Total Elongation (SRs from 10^{-1} to 10^{-6} s^{-1})	1	**
Uniform Elongation (SRs from 10^{-1} to 10^{-6} s^{-1})	1	
UTS at 25°C	1	**
Yield Strength (SRs from 10^{-1} to 10^{-6} s^{-1})	1	**
Hardness	3	**
Work Hardening Coefficient (SRs from 10^{-1} to 10^{-6} s^{-1})	1	**
Creep Resistance (SRs from 10^{-1} to 10^{-6} s^{-1})	1	**
Min. Creep Strain rate at Stress of 20MPa at R°	1	**
Min. Creep Strain rate at Stress of 20MPa at 125°C	1	**
Thermomechanical Fatigue resistance(SRs from 10^{-1} to 10^{-6} s^{-1})	1	
Isothermal Fatigue Data (SRs from 10^{-1} to 10^{-6} s^{-1})	1	
Thermal Fatigue Hysteresis behaviour(SRs from 10^{-1} to 10^{-6} s^{-1})	1	
Constitutive Behavior(SRs from 10^{-1} to 10^{-6} s^{-1})	1	**
Stress Rupture(SRs from 10^{-1} to 10^{-6} s^{-1})	3	**
Dynamic Acoustic Measurements	3	
Fracture Toughness at R° (SRs from 10^{-1} to 10^{-6} s^{-1})	3	

1 = high Priority, 2 = medium priority, 3 = low priority

* Existing features of JMatPro

** Features to be implemented in the near future

References

1 U.R. Kattner, *JOM*, December, (2002), 45-51.

2. X.J. Liu I. Ohnuma, C.P. Wang, M. Jiang, R. Kainuma, K. Ishida, M. Ode, T. Koyama, H. Onodera and T. Suzuki, *J. Electron. Mater.*, 32, (2003), 1265-1272.
3. Z. Moser, W. Gasior, J. Pstrus, S. Ishihara, X.J. Liu and I. Ohnuma, *Mater. Trans.*, 45, (2004), 652-660.
4. N. Moelans, K.C. Hari Kumar and P. Wollants, *J. Alloys & Compounds*, 360, (2003), 98-106.
5. S.W. Yoon, J.R. Soh, H.M. Lee and B.J. Lee, *Acta Mater.*, 45, (1997), 951-960.
6. N. Saunders, Z. Guo, X. Li, A.P. Miodownik and J.P. Schillé, *JOM*, December, (2003), 60-65.
7. N. Saunders, *Aluminium Alloys, Their Physical and Mechanical Properties*, eds. J.F. Nie et al. (Melbourne, Australia: Inst. Mater. Eng. Australasia), 96.
8. X. Li, A.P. Miodownik and N. Saunders, *Mater. Sci. Tech.*, 18, (2002), 861.
9. N. Saunders, Z. Guo, X. Li, A.P. Miodownik and J.P. Schillé, Superalloys 2004 (10th International Symposium on Superalloys, 19-23 September, 2004, Champion, Pennsylvania), eds. K. Green et al. (Warrendale, PA: TMS, 2004), 849-858.
10. N. Saunders, X. Li, A.P. Miodownik and J.-Ph.Schillé, Ti-2003 Science and Technology, eds. G. Luetering and J. Albrecht, (Weinheim, Germany: Wiley-VCH, 2004), 1397-1404.
11. L. Kaufman and H. Bernstein, *Computer Calculations of Phase Diagrams*, (New York: Academic Press, 1970)
12. N. Saunders and A.P. Miodownik, *CALPHAD – Calculation of Phase Diagrams*, *Pergamon Materials Series vol.1*, ed. R.W. Cahn, (Oxford: Elsevier Science, 1998).
13. T. Siewert, S. Liu, D.R. Smith, and J.C. Madeni, *Properties of Lead-Free Solders, Release 4.0*, (NIST and Colorado School of Mines, 2002) http://www.boulder.nist.gov/div853/lead%20free/solders.html
14. Z. Fan, P. Tsakiropoulos and A.P. Miodownik, *J. Mat. Sci.*, 29 (1994) 141.
15. Z. Fan, *Phil. Mag. A*, 73 (1996), 1663.
16. A.P. Miodownik, N. Saunders and J.P. Schillé, *unpublished research.*
17. N. Saunders, X. Li, A.P. Miodownik and J.P. Schillé, *Modelling of Casting, Welding and Advanced Solidification Processes X*, eds. D. Stefanescu, J.A. Warren, M.R. Jolly and M.J.M. Krane (Warrendale, PA: TMS, 2003**)**, 669-676.
18. P.T. Vianco, Sandia Laboratories (2001) as given in ref. [13].
19. J.A.V. Butler, *Proc. Roy. Soc A*, 135, (1932), 348.
20. T. Tanaka, K. Hack and S.Hara, *MRS Bull.*, April, (1999), 45.
21. J.H. Lee and D.N. Lee, *J. Electron. Mater.*, 30, (2001), 1112.
22. W. Gasior, Z. Moser and A. Debski., *Arch. Metall. & Mat.*, 49, (2004), 575.
23. R. Picha, J. Vrestal and A. Kroupa, *CALPHAD,* 28, (2004), 141.
24. G. Metzger, Z. Phys. Chem, 211, (1959), 1.
25. J.C. Joud, N. Eustathopoulos, A. Bricard and P. Desre, J. Chem. Phys., 70, (1973), 1290.
26. R. Pajarre, P. Koukkari, T. Tanaka and J. Lee, *CALPHAD*, 30, (2006), 196.
27. T. Tanaka and T. Iida, *Steel Research*, 65, (1994), 21.
28. K. Mori, M. Kishimoto, T. Shimose and Y. Kawai, *J. Jap. Inst. Metals*., 39, (1975), 1301.
29. X.J. Liu,Y. Inohana, I. Ohnuma, R. Kainuma, K. Ishida, Z. Moser, W. Gasior and J. Pstrus, *J. Electron. Mater.*, 31, (2002), 1139.
30. A.P. Miodownik *in preparation*
31. http://www.nemi.org/cms/newsroom/Presentations/lf_workshop_report.html